Characterization of dam breaching following overtopping

Ana Margarida Bento
ana.bento@ist.utl.pt

November 4, 2013

Abstract

Bearing in mind the scope of the present paper, the overall objective is the characterization of effluent hydrographs caused by overtopping failures of earth dams. Two laboratory experiments on homogeneous embankments (h_{dam} = 45/48 cm) were performed in a medium scale facility of National Laboratory of Civil Engineering (LNEC). Suitable instrumentation and measurement methods enabled two indirect and one direct estimation of the breach effluent hydrograph. Different compaction energies and different pilot channel geometries were used. The resultant hydrographs show that the surface erosion is the main mechanism for breach enlargement, although key features such as sudden increase are explained by localized mass instability events.

Keywords: overtopping, dam-breach, effluent hydrograph, LSPIV

1 Introduction

The large benefit of dams to people worldwide is well known. Nevertheless, the large quantities of water suddenly released and the consequences of dam failure, such as the property damage and the loss of life, are all of prime importance to our society (Wahl, 1998). A dam-break flood event may also cause adverse ecological and environment impact upstream and downstream of the dam. In Portugal, the failure of the Fonte Santa mine tailings dam generated a flood wave that caused significant morphological changes in the valley of Ribeira da Fonte Santa, tributary of Rio Sabor, mostly due to the deposition of muds contaminated with metals from mine washing.

According to ICOLD (2013), 75 % of the dams in service around the world are embankment dams, which can also be divided in 'earth fill' and 'rock fill' dams, depending on whether it is comprised of compacted earth or mostly compacted of dumped rock, respectively.

From all the causes of dam failures, overtopping phenomenon constitutes the most common in embankment dams. According to ICOLD (2013), it represents 35 % of all embankment failures in the world. Thus and due to the impossibility of completely eliminate that risk, the challenge lies on understanding how the dam behaves face to an overtopping failure.

Therefore, the purpose of this work is to quantify the breach hydrograph resulting from overtopping of an homogeneous earth dam and to discuss the inherent hydraulic and geotechnical phenomena. Two dam-breach experiments on homogeneous embankments are performed to further the understanding of the breach mechanisms underlying the interaction between the fluid flow and the dam material.

In order to ensure adequate hydraulic and mechanical properties for the soil and homogeneity of the embankments, two trial embankments were performed, varying the compactor, energy of compaction and the layer thickness.

2 Dam-breach experiments

2.1 Experimental set-up

2.1.1 Facilities

The dam-breach experiments were conducted in a channel 31.5 m long, between 6.60 - 1.70 m wide and between 0.5 - 1.30 m deep. At 17.7 m from the reservoir inlet, vertical concrete walls (0.5 m height) were built to narrow the length of the dam crest of the embankment models (1 m for the first experiment and 1.5 m for the second experiment - see figure 9 and 10). The reservoir filling did not required special care with wave development due to its high capacity. The channel filling was performed by a pumping system, which as a flow controller with 200 l/s as maximum capacity (two pumps - 100 l/s each). Water was pumped from a storage tank (with approximately 90 m^3/s of maximum stored volume) to another tank located above the pumping room where it was transported, by gravity, to the reservoir by a pipe with 350 mm diameter. This channel had an antechamber separated from the main channel by a hollow brick wall to curb large turbulent scales and evenly distribute the flow towards the embankments. At the end of the channel was located a settling basin with 1.7 m width, 4.5 m length and a maximum water/sediments height of approximately 0.60 m. For the second experiment, two lateral spillways, 2.5 m long, were performed with the aim of improving the control/measurement of the temporal variation of the reservoir water level.

2.1.2 Earth embankments

The embankment models built to perform the two dam-breach experiments used only one type of soil. The specific gravity (G_s) was measured with a pycnometer ($G_s = 2.64$). The grain-size distribution curve was built from sieve and sedimentation analysis and is shown in figure 1.

According to the soil fractions (see table 1) and using the Unified Soil Classification System, the soil was classified as SM-silty sand.

Table 1: Soil fractions of the soil in study.

Soil Fractions (%)		
Gravel	Sand	Fines
6.8	66.0	27.2

Soil water content ($w_{optimum}$) and maximum dry volumetric weight (γ_d) were determined by two proctor compaction curves performed according to Especificação (1966). The Proctor curves obtained are shown in figure 2. The optimal parameters of the Proctor tests are given in table 2.

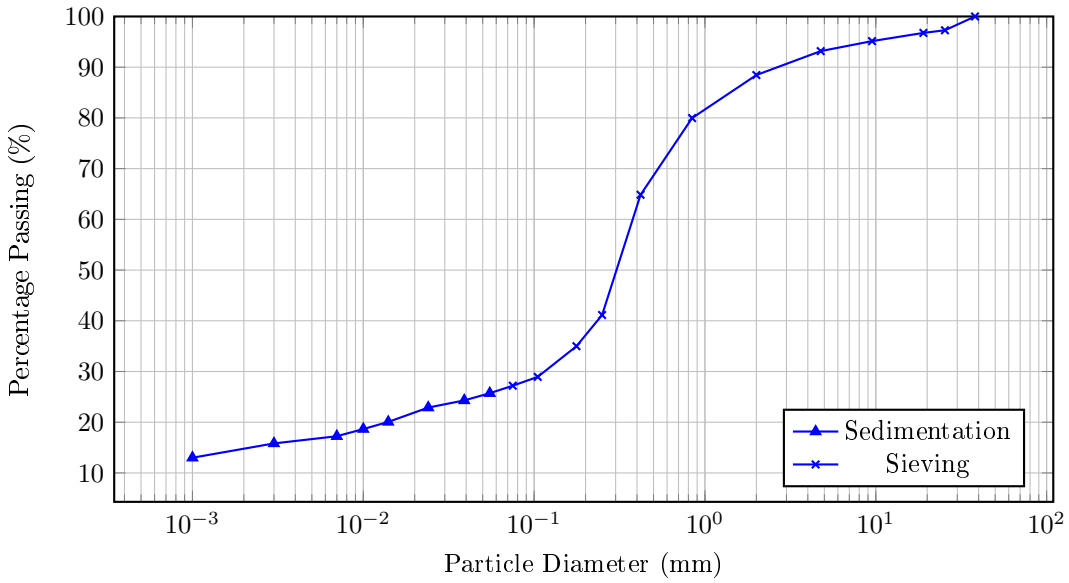

Figure 1: Grain-size distribution curve of the soil in study.

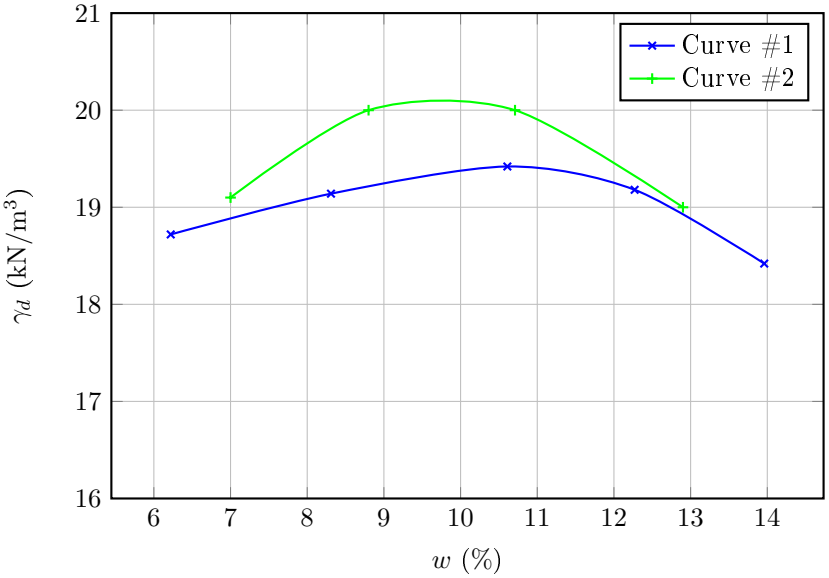

Figure 2: Proctor curves.

Table 2: Optimal parameters of Proctor tests.

Curve	γ_d (kN/m^3)	$w_{optimum}$ (%)
#1	20.1	9.7
#2	19.4	10.6
Average	19.8	10.2

The Proctor curves are not coincident, which may be explained by some unavoidable heterogeneity of the soil. Average values of maximum dry volumetric weight and optimum water content were adopted for compaction control. Thus, the optimum water content and the dry volumetric weight considered in compaction control are 10.2% and 19.8kN/m^3, respectively.

Before the dam construction, two trial embankments were performed to ensure a proper compaction of them. The first trial embankment was performed using a wood rod with a sheaf coupled to a wood plate at a bottom with a 10 cm layer thickness and the second was performed by a slick roller without vibration. Further details are given in Bento (2013).

The embankments of each dam-breach experiment were, therefore, performed using the compactor of the 1^{st} trial embankment (see figure 3), although applying different compaction energies. The first considered four blows in each layer whilst in the second twelve blows were applied in order to study the density effects. For the type of soil in study, it was specified that the degree of compaction for the second embankment should show a minimum of 85% and a water content within the interval $w \in [w_{optimum}, w_{optimum} + 2\%]$.

Figure 3: Compactor of the 1^{st} trial embankment.

The dams built incorporated a multiple stage system to ensure a uniformity and an accurate compaction. Each construction stage involved the placement of an equal material thickness of soil (10 cm) to which some water was added until the soil showed the right amount of water content for proper compaction (using the "Hand Test" as reference being this test always performed by the same person). Then, they were shaped in order to achieve the proper upstream and downstream slopes. Shaping was done using a set-square as a trowel to ensure the uniformity of the slope (Figure 4 and 5), for each embankment). At the middle of the embankment crest, an initial rectangular shaped breach section of 0.10 m wide and 0.055 m high was carved for the first. For the second embankment, an initial triangular shaped breach section was considered. This was done not only to control the area of concentrated flow and the initial erosion at the beginning of the overtopping phenomenon, but also to mitigate the effects of the side walls of the channel, where the experiments were performed. The embankments geometry, for each dam-breach experiment, are illustrated below in figures 4 and 5.

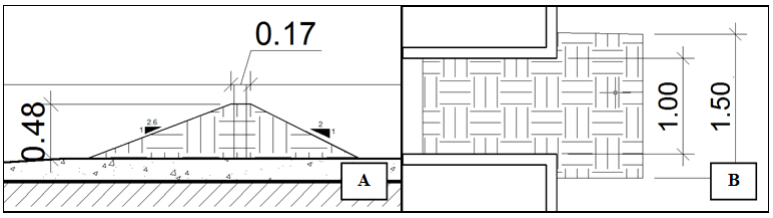

Figure 4: Dimensional scheme of the first embankment.

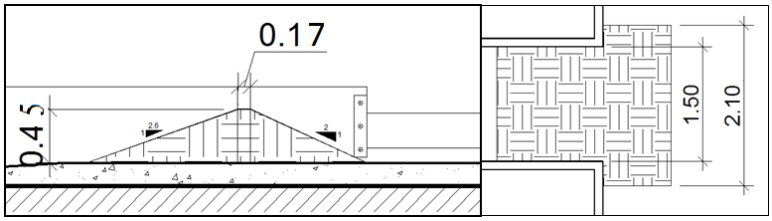

Figure 5: Dimensional scheme of the second embankment.

The initial breach geometries of each embankment are shown in figures 6 and 8, respectively.

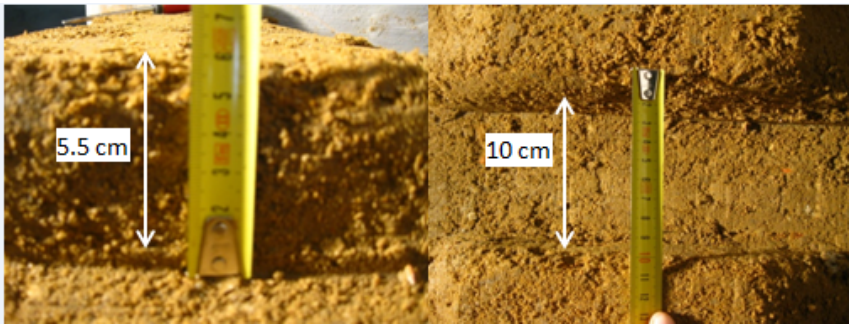

Figure 6: Geometry of the pilot channel of the first embankment.

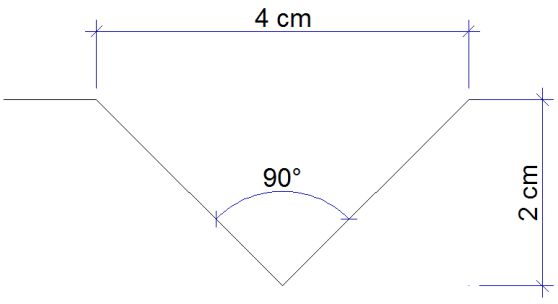

Figure 7: Dimensional scheme of the pilot channel of the second embankment.

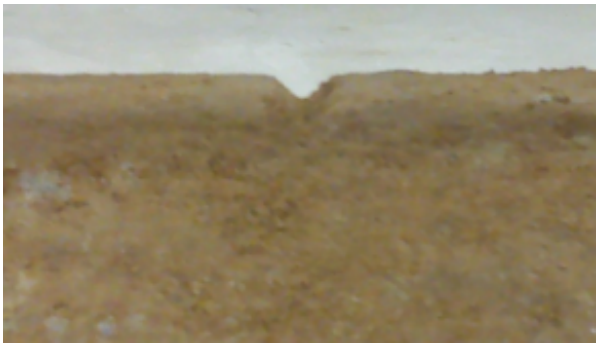

Figure 8: Photo of the pilot channel of the second embankment.

2.1.3 Instrumentation

A set of reliable instrumentation for measuring the variations of the inflow discharge as well as the water elevation within the reservoir and downstream the embankment during the first dam-breach experiment was applied. These measurements were possible using a digital electromagnetic flowmeter and water level

probes - three resistive and four acoustic probes, respectively (see figure 9 for their positions). Two digital video cameras, also shown in figure 9, were used to record the breach events: one located downstream of the embankment and the other one above the crest looking down at the embankment.

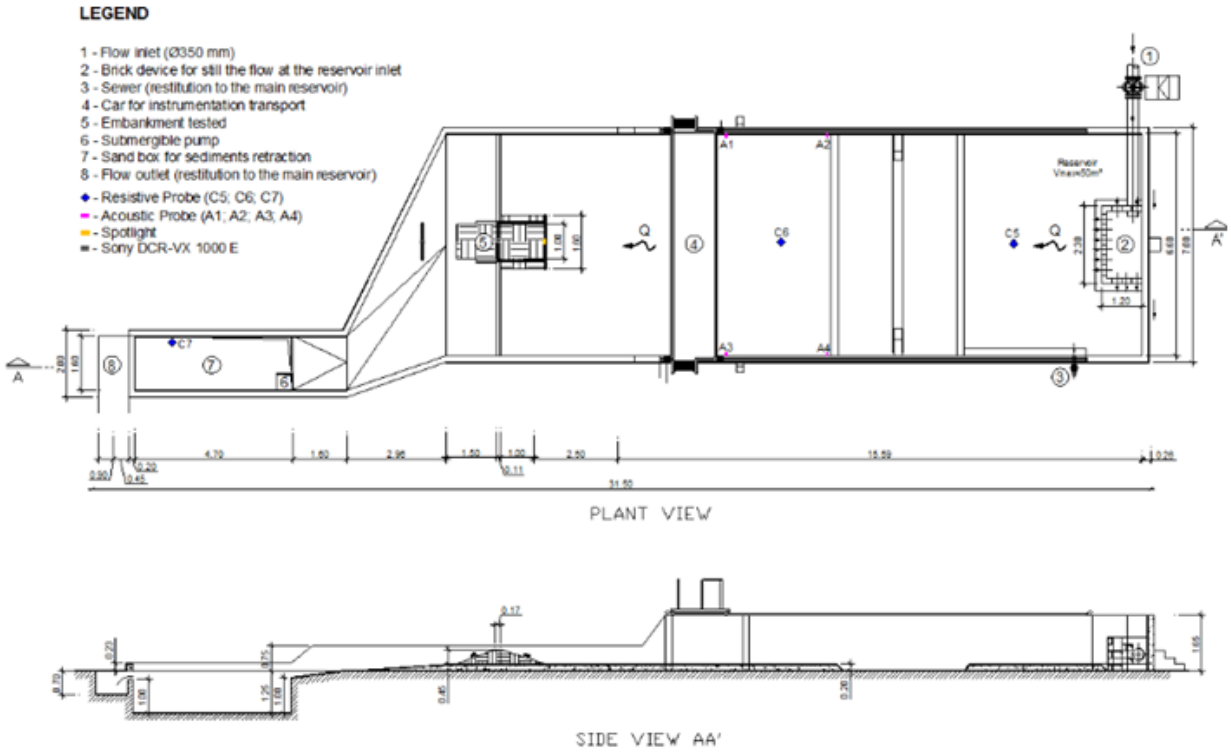

Figure 9: General view of the channel and the instrumentation used in the first dam-breach experiment.

The experimental data of the second dam-breach experiment were obtained using five different types of instrumentation, located in strategic places. They comprised a flowmeter, four resistive probes, two limnimeters, two high-speed video cameras and one digital video camera. These instrumentation were situated upstream and downstream of the dam (see figure 10).

The flowmeter enabled the control of the discharge entering in the channel. The mission of the acoustic probes, resistive probes and the limnimeters was twofold: to take water level measurements within the reservoir (and near the downstream spillway) during the test and to enable the calculation of the outflow discharge through the breach by means of appropriate hydraulic concepts and relationships. The digital video camera, placed at the downstream side of the dam, had the intuit of obtaining a frontal profile of the breach formation and its evolution during the overtopping failure. The digital camera placed above the crest, looking down at the embankment, allowed an overhead profile of the dam breaching phenomenon. See figure 9 for details.

The two high-speed video cameras (indicated in figure 10) allowed a direct quantification of velocities over the breach, with a LSPIV algorithm, and the estimation of the breach cross-section area. In order to properly analyse those images, two additional instruments were used: styrofoam beads as flow tracers, and a 8W laser, respectively. For a detailed description about the calibration and the operation of these measurement instrumentation see Bento (2013).

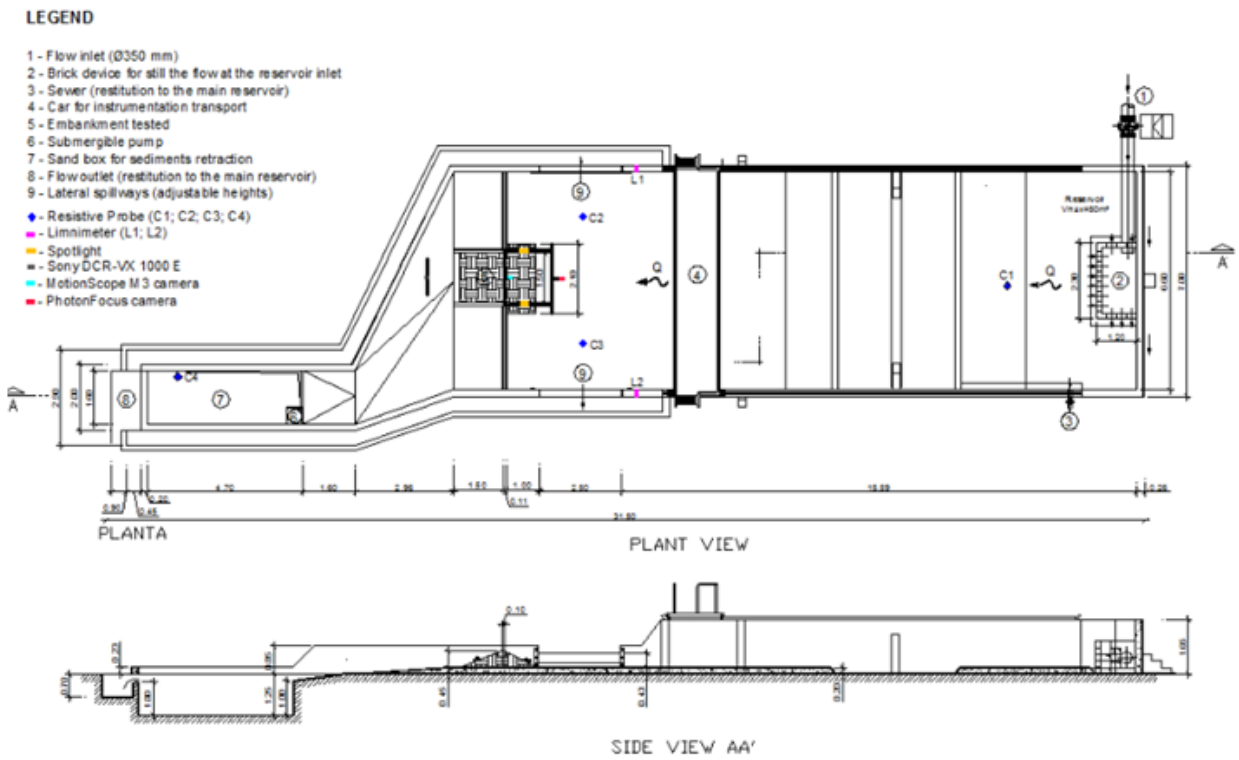

Figure 10: General view of the channel and the instrumentation used in the second dam-breach experiment.

3 Experimental results

Before the estimation of the breach effluent hydrographs was necessary to perform a brief sensitivity analysis to noise reduction techniques. The data from the water elevation probes showed high level of background noise, that needed a reduction. Therefore, a digital filter and a local average technique were used to improve the reliability of the data.

The instrumentation used for the first dam-breach experiment allowed two indirect estimations of the breach effluent hydrographs. These estimations were based on the mass balance equation (Equation 1) and on the calibration curve of the downstream spillway. The first had additionally the ability to consider a simple or a weighted contribution of the probes used in each experiment (applying the Voronoi polygons within the reservoir).

$$\frac{d\forall}{dt} = Q_{in}(t) - Q(t) \tag{1}$$

The second estimation, based on the calibration curve of the downstream spillway, showed good results only for lower discharge values, due to the limited interval of the curve applicability.

For the second dam-breach experiment, a new and robust instrumentation allowed, beyond these indirect ways, a direct estimation of the breach effluent hydrograph. This estimation was based on the direct quantification of the flow velocity, with a LSPIV algorithm, and on the estimation of the breach cross-section area, both with the aid of the two high-speed video cameras used.

The breach effluent hydrographs obtained for each dam-breach experiments are represented below (Figure 11 and 12, respectively).

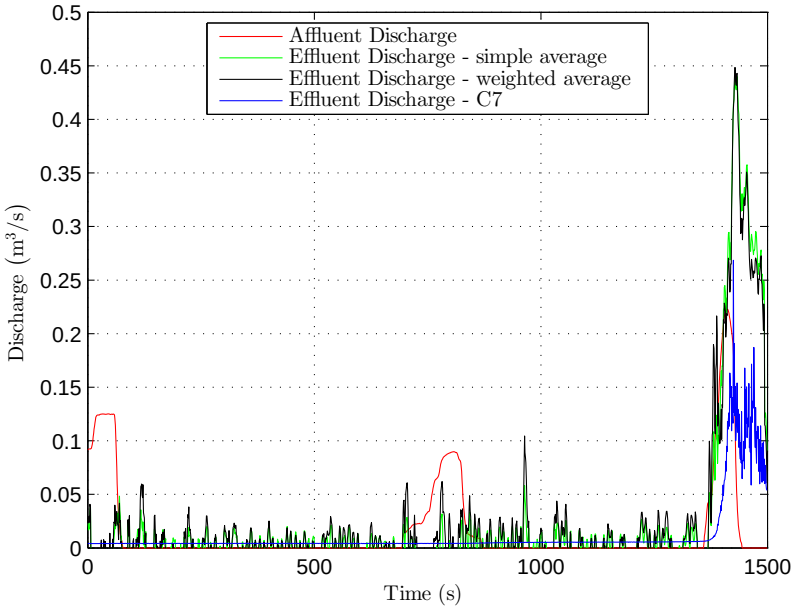

Figure 11: Breach effluent discharge estimations of the first experiment.

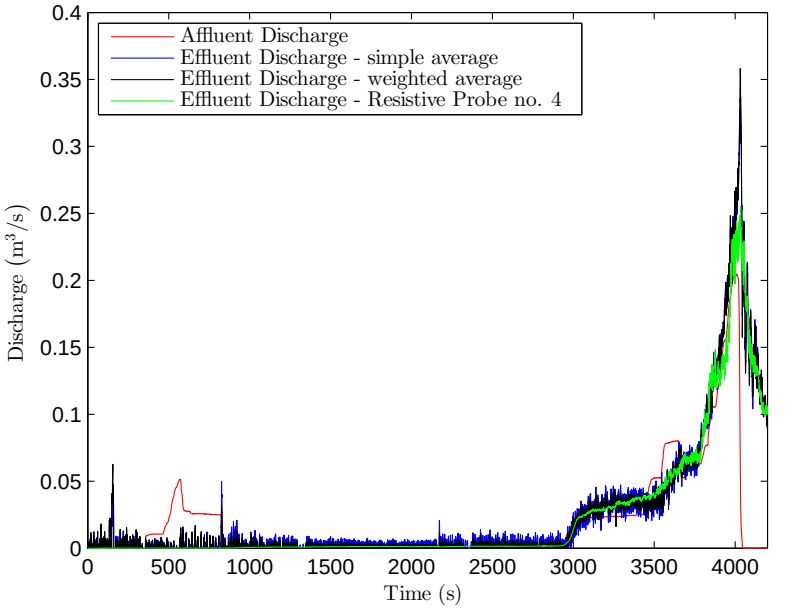

Figure 12: Breach effluent discharge estimations of the second experiment.

These two plots show different behaviours. In the first (Figure 11) is evident a very rapid breaching development, with the detachment of large masses of soil, which evolved to a relatively large size of the final breach. In this case, the effluent discharge reached a peak in a very short time and then the hydrograph suffered a dramatic drop. This result may be a result of the low compaction energy applied during the respective embankment construction.

The hydrograph of the second experiment (Figure 12), using another energy of compaction and another initial geometry for the pilot channel showed a slow increase of the effluent discharge and a peak discharge

of less magnitude, when compared to the obtained in the first experiment.

The direct estimation of the effluent discharge for the second dam-breach experiment, represented in figure 13, shows a very similar behaviour to the indirect estimations, although for only a restricted temporal interval was possible to perform that estimation.

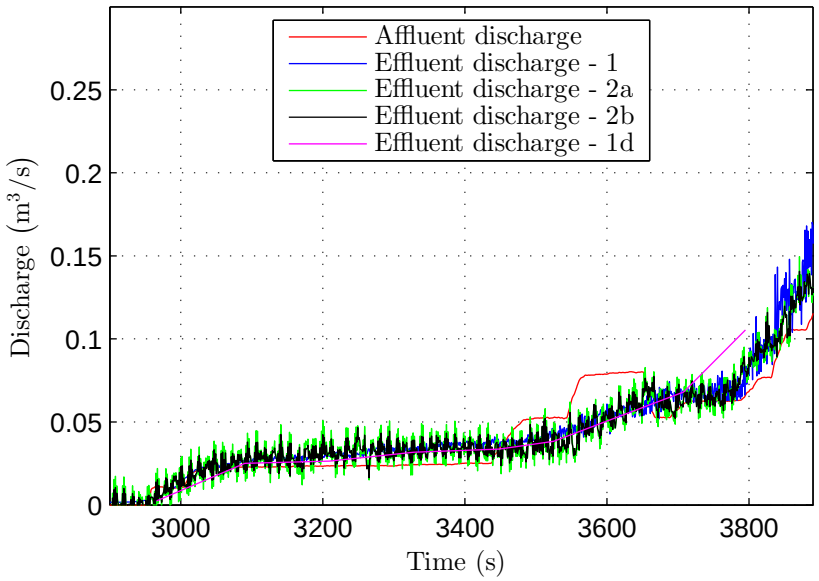

Figure 13: Comparison between the indirect estimations and the direct estimation (1d).

Acknowledgements

I would like to express appreciation to my supervisor, Prof. Rui M. L. Ferreira, and my co-supervisor, Prof. Rafaela Cardoso, for their continuous support and guidance during this work.

References

Bento, A. M. (2013). *Characterization of dam breaching following overtopping.* Master's thesis, Instituto Superior Técnico.

Especificação, L. (1966). E197, solos. *Ensaio de compactação, LNEC, Lisboa* .

ICOLD (2013). Technology of dams.

Wahl, T. (1998). Prediction of embankment dam breach parameters: a literature review and needs assessment .